Loop Shaping Controller Design for Constant Output Interleaved Boost Converter using Real-Time Hardware in-the-Loop(HIL)

Vaishali Chapparya, G. Murali Krishna,
Prakash Dwivedi, *Member, IEEE*, and Sourav Bose, *Member, IEEE*

***Abstract*—Numerous control techniques have been reported in literature to enhance the performance of interleaved boost converter(IBC), which is intrinsically a non minimal phase system. The present study puts forward a novel graphical loop shaping technique for designing a controller for non minimal phase IBC. The stability analysis of the open loop and closed loop IBC are carried out using MATLAB environment. Further to validate the efficiency of the proposed controller the real-time hardware in-the-loop (HIL) emulation is carried out using Typhoon HIL 402.**

***Index Terms*—Non-Minimal Phase System (NMP), Interleaved Boost Converter, Loop Shaping, Hardware in-the-Loop (HIL).**

I. Introduction

Wide usage of non renewable sources of energy like coal, oil, natural gas e.t.c., has resulted into pollution. The major demerit of non renewable source of energy is once consumed, it cannot be replenished. Thus renewable sources of energy like wind, solar, hydro e.t.c., came into picture. The power generation from renewable source of energy require low maintenance cost.

It has been found that boost converters are frequently used for increasing the voltage level but the presence of ripple in current and output voltage, may lead the converter into discontinuous mode conduction [1]. To reduce the ripples in source current and output voltage, an IBC was introduced. Interleaving technique is slightly different paralleling technique. In this technique switching instants are phase shifted over a switching period. Equal phase shift among the parallel power stages reduce the output capacitor ripple [2]. Interleaving provides with better power capability, efficiency[3], faster dynamics, light weight and high power density [4], reliability [5], improved input current, output voltage and inductor current ripple characteristics[6]. IBC has various industrial applications such as in power factor correction circuits [7], [8], photovoltaic system [9], fuel cell systems [10].

IBC posses NMP behaviour and inherently open loop unstable thus making the design of a controller for stabilization of IBC a difficult task. The design and mathematical modelling becomes much more complex when large number of elements are present in converter circuit [11], [12].

Various control strategies have been proposed in the literature to design a controller for IBC such as Sic MOSFET and Fuzzy Logic Controller [13], PSO-Based Type-III Controller [14], Robust Model Predictive Control [15], 2DOF digital controller [16], Type III Controller [17], Robust STATCOM Voltage Controller Design [18]. Each of these strategies demand complex computations due to its manifold structure.

Here author suggests a graphical loop shaping technique to design a controller for non-minimal phase IBC system. The central idea of the method is to construct the loop transfer function L graphically to fulfill the robust performance criterion, and then controller is realized using the transfer function from the magnitude curve of plant and magnitude curve of loop transfer function. The time & frequency response of IBC with and without proposed controller is simulated in MATLAB environment. Further the real-time implementation is done using Typhoon HIL 402 device.

The paper is organized as follows.The mathematical modelling with different modes of operation of the interleaved boost converter, transfer function of output to perturbed duty cycle is given in Section 2. In Section 3, controller design using loop shaping technique is discussed. Results and discussion is presented in Section 4. Conclusions follow in the last section of this paper.

II. Interleaved Boost Converter

A. Experimental Framework

Interleaved boost converter works like two boost converters are connected in parallel and its circuit diagram is shown in Fig. 1. IBC is having four modes of operation as mentioned in Table I. In IBC, to get the symmetrical operation of two parallel paths switches S1 and S2 are triggered with identical gate pulse signals G1 and G2. There should be a delay of half cycle between these two pulses. However, three modes of operation will be notified out of the four modes, dependent on the value of duty ratio(D). If $D < 0.5$ the converter operates in modes 2, 3, 4 and if $D > 0.5$ converter operates in modes 1, 2, and 3.

B. Governing Equations

The mathematical modelling of the IBC in all four modes is carried out for getting average state space model. The state variables chosen are i_{l1}, i_{l2} and V_c.

Mode-1: The circuit diagram of mode-1 operation of IBC is shown in Figure 2. Applying KVL , KCL in Figure 2 and

Vaishali Chapparya, Department of Electrical Engineering, National Institute of Technology, Uttarakhand, India. e-mail:vaishali932s@rediffmail.com
G.Murali Krishna, Department of Electrical Engineering, National Institute of Technology, Uttarakhand, India. e-mail:muralikrishnagowra@gmail.com
Prakash Dwivedi, Department of Electrical Engineering, National Institute of Technology, Uttarakhand, India. e-mail:prakashdwivedi@nituk.ac.in
Sourav Bose, Department of Electrical Engineering, National Institute of Technology, Uttarakhand, India. e-mail:souravbose@nituk.ac.in

ISBN: 978-988-14048-8-6
ISSN: 2078-0958 (Print); ISSN: 2078-0966 (Online)

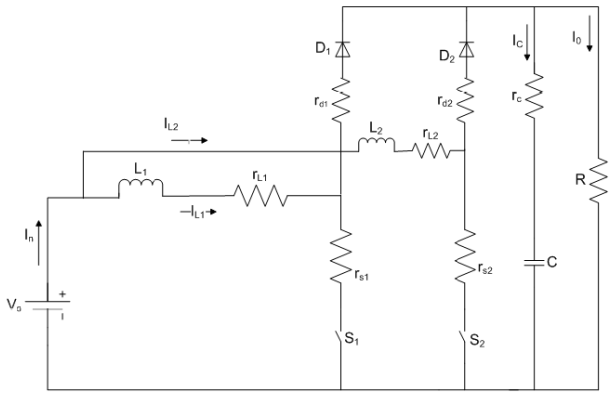

Fig. 1: Circuit diagram of IBC

TABLE I: Different Modes of operation of IBC

S_1	S_2	Mode
ON	ON	Mode - 1
ON	OFF	Mode - 2
OFF	ON	Mode - 3
OFF	OFF	Mode - 4

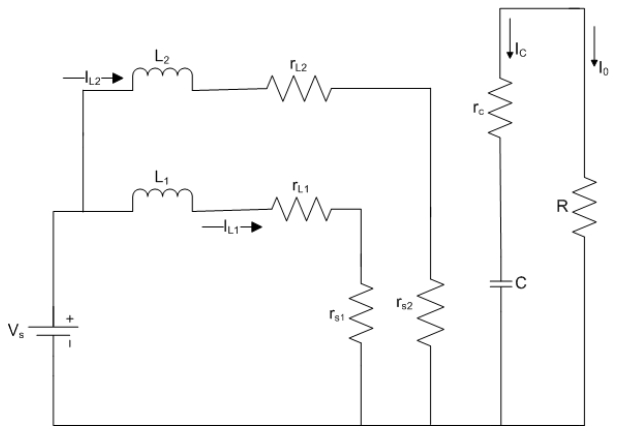

Fig. 2: Mode-1 operation of IBC

rearranging further will yield Eq. (1), (2), (3), and (4).

$$\frac{\mathrm{d}i_{L1}}{\mathrm{d}t} = \frac{V_s}{L_1} - \frac{i_{l1}(r_{l1}+r_{s1})}{L_1} \tag{1}$$

$$\frac{\mathrm{d}i_{L2}}{\mathrm{d}t} = \frac{V_s}{L_2} - \frac{i_{l2}(r_{l2}+r_{s2})}{L_2} \tag{2}$$

$$\frac{\mathrm{d}V_c}{\mathrm{d}t} = \frac{-V_c}{C(r_c+R)} \tag{3}$$

$$V_o = \frac{RV_c}{(r_c+R)} \tag{4}$$

Using Eq. (1) to (4) the state space model of mode-1 operation is given in Eq. (5) & (6)

$$\begin{bmatrix} \dot{i_{l1}} \\ \dot{i_{l2}} \\ \dot{V_c} \end{bmatrix} = \begin{bmatrix} -\frac{(r_{l1}+r_{s1})}{L_1} & 0 & 0 \\ 0 & -\frac{(r_{l2}+r_{s2})}{L_2} & 0 \\ 0 & 0 & -\frac{1}{C(R+r_c)} \end{bmatrix} \begin{bmatrix} i_{l1} \\ i_{l2} \\ V_c \end{bmatrix} + \begin{bmatrix} \frac{1}{L1} \\ \frac{1}{L2} \\ 0 \end{bmatrix} V_s \tag{5}$$

$$V_o = \begin{bmatrix} 0 & 0 & \frac{R}{R+r_c} \end{bmatrix} \begin{bmatrix} i_{l1} \\ i_{l2} \\ V_c \end{bmatrix} \tag{6}$$

Similarly the state space models of other modes of operation are obtained and given in Eq. (7) to (12).

Mode-2:

$$\begin{bmatrix} \dot{i_{l1}} \\ \dot{i_{l2}} \\ \dot{V_c} \end{bmatrix} = \begin{bmatrix} -\frac{(r_{l1}+r_{s1})}{L_1} & 0 & 0 \\ 0 & -\frac{(r_{l2}+r_{d2}+\frac{Rr_c}{R+r_c})}{L_2} & -\frac{R}{(R+r_c)L_2} \\ 0 & +\frac{R}{C(R+r_c)} & -\frac{1}{C(R+r_c)} \end{bmatrix} \begin{bmatrix} i_{l1} \\ i_{l2} \\ V_c \end{bmatrix} + \begin{bmatrix} \frac{1}{L1} \\ \frac{1}{L2} \\ 0 \end{bmatrix} V_s \tag{7}$$

$$V_o = \begin{bmatrix} 0 & \frac{Rr_c}{R+r_c} & \frac{R}{R+r_c} \end{bmatrix} \begin{bmatrix} i_{l1} \\ i_{l2} \\ V_c \end{bmatrix} \tag{8}$$

Mode-3:

$$\begin{bmatrix} \dot{i_{l1}} \\ \dot{i_{l2}} \\ \dot{V_c} \end{bmatrix} = \begin{bmatrix} -\frac{(r_{l1}+r_{d1}+\frac{Rr_c}{R+r_c})}{L_1} & 0 & 0 \\ 0 & -\frac{(r_{l2}+r_{s2})}{L_2} & 0 \\ \frac{R}{C(R+r_c)} & 0 & -\frac{1}{C(R+r_c)} \end{bmatrix} \begin{bmatrix} i_{l1} \\ i_{l2} \\ V_c \end{bmatrix} + \begin{bmatrix} \frac{1}{L1} \\ \frac{1}{L2} \\ 0 \end{bmatrix} V_s \tag{9}$$

$$V_o = \begin{bmatrix} \frac{Rr_c}{R+r_c} & 0 & \frac{R}{R+r_c} \end{bmatrix} \begin{bmatrix} i_{l1} \\ i_{l2} \\ V_c \end{bmatrix} \tag{10}$$

ISBN: 978-988-14048-8-6
ISSN: 2078-0958 (Print); ISSN: 2078-0966 (Online)

Mode-4:

$$\begin{bmatrix} \dot{i_{l1}} \\ \dot{i_{l2}} \\ \dot{V_c} \end{bmatrix} = \begin{bmatrix} -\frac{(r_{l1}+r_{d1}+\frac{Rr_c}{R+r_c})}{L_1} & -\frac{Rr_c}{(r_c+R)L_1} & -\frac{R}{(r_c+R)L_1} \\ -\frac{Rr_c}{(r_c+R)L_2} & -\frac{(r_{l2}+r_{d2}+\frac{Rr_c}{R+r_c})}{L_2} & -\frac{R}{(r_c+R)L_2} \\ \frac{R}{C(R+r_c)} & \frac{R}{C(R+r_c)} & -\frac{1}{C(R+r_c)} \end{bmatrix} \begin{bmatrix} i_{l1} \\ i_{l2} \\ V_c \end{bmatrix} + \begin{bmatrix} \frac{1}{L1} \\ \frac{1}{L2} \\ 0 \end{bmatrix} V_s \quad (11)$$

$$V_o = \begin{bmatrix} \frac{Rr_c}{R+r_c} & \frac{Rr_c}{R+r_c} & \frac{R}{R+r_c} \end{bmatrix} \begin{bmatrix} i_{l1} \\ i_{l2} \\ V_c \end{bmatrix} \quad (12)$$

C. Averaging & Small Signal Analysis

To achieve final state space space of the converter using state space matrices of various modes of operation mentioned in previous section (Eq. (5) to (12)), averaging is required. Therefore, this section deals with averaging & small small signal analysis.

The average matrices A, B, C are given in Eq. (13), (14), (15) for D $<$ 0.5.

$$A = D(A_2 + A_3) + (1 - 2D)A_4 \quad (13)$$

$$B = D(B_2 + B_3) + (1 - 2D)B_4 \quad (14)$$

$$C = D(C_2 + C_3) + (1 - 2D)C_4 \quad (15)$$

Similarly the average matrices A, B, C are given in Eq. (16), (17), (18) for D $>$ 0.5.

$$A = (1 - D)(A_2 + A_3) + (2D - 1)A_1 \quad (16)$$

$$B = (1 - D)(B_2 + B_3) + (2D - 1)B_1 \quad (17)$$

$$C = (1 - D)(C_2 + C_3) + (2D - 1)C_1 \quad (18)$$

where A_1, A_2, A_3, A_4 are the system matrices of the respective modes of operation. Similarly B_1, B_2, B_3, B_4 are the input matrices and C_1, C_2, C_3, C_4 are the output matrices.

The final average state space equation of the converter are as given in Eq. (19) and (20).

$$\dot{X} = AX + BV_s \quad (19)$$

$$V_o = CX \quad (20)$$

The average state space matrices obtained in Eq. (19) and (20) are dealing with steady state response. The deviations present around the steady state are not considered in the above equations. The small signal analysis is a way to include the deviations in state space modelling.

Adding deviations as d = D + $\hat{d}$, x = X + $\hat{x}$, v_s = V_s + $\hat{v_s}$ and simplifying Eq. (19) is rearranged as Eq. (21)

$$\hat{\dot{x}} = A\hat{x} + B\hat{v_s} + [((A_2+A_3)-2A_4)X + ((B_2+B_3)-2B_4)V_s]\hat{d} \quad (21)$$

Laplace transform of Eq. (21) is given in Eq. (22)

$$\hat{x}(s) = [sI - A]^{-1}B\hat{v_s} + [sI - A]^{-1}[((A_2 + A_3) - 2A_4)X + ((B_2 + B_3) - 2B_4)V_s]\hat{d}(s) \quad (22)$$

Equation (23) is obtained after substituting $B\hat{v_s} = 0$ and defining M = $[(A_2 + A_3) - 2A_4]$, N = $[(B_2 + B_3) - 2B_4]$ in Eq. (22)

$$\hat{x}(s) = [sI - A]^{-1}[(M)X + (N)V_s]\hat{d}(s) \quad (23)$$

Similarly adding deviations in D, X, V_s and simplifying Eq.(20) is modelled into Eq.(24)

$$\hat{v_o}(s) = [(C_2 + C_3 - 2C_4)X]\hat{d}(s) + C\hat{x}(s) \quad (24)$$

Defining K = $C_2 + C_3 - 2C_4$ and substituting in above equation, Eq.(25) is obtained

$$\hat{v_o}(s) = [C]\hat{x}(s) + [KX]\hat{d}(s) \quad (25)$$

Substituting value of $\hat{x}(s)$ from Eq.(23) in Eq.(25) yields Eq. (26)

$$\hat{v_o}(s) = C[sI - A]^{-1}[[M]X + [K]X + [N]V_s]\hat{d}(s) \quad (26)$$

Thus the final transfer function of output to perturbed duty cycle can be expressed as given in Eq.(27)

$$\frac{\hat{v_o}(s)}{\hat{d}(s)} = C[sI - A]^{-1}[[M]X + [K]X + [N]V_s] \quad (27)$$

Similarly the transfer function can be achieved for D $>$ 0.5.The input, output design requirements and calculated inductor and capacitor values are tabulated in Table II. Substituting these values in Eq.(27), the tranfer function of IBC is obtained as given in Eq.(28).

$$\frac{\hat{v_o}(s)}{\hat{d}(s)} = \frac{82.5(1 + s/17.85 * 10^6)(1 - s/1238.15)}{(1 + s/2377.45)(1 + s/2624.49)} = G(s) \quad (28)$$

III. Controller Design

The transfer function mentioned in Eq. (28) depicts a zero in right half of s plane which represents the non-minimal phase characteristic of the IBC.

Number of controllers has been proposed for the interleaved boost converter in [9],[16],[19], [20]. In the present paper, "Loop Shaping" design technique is implemented. This technique demands less computation and give efficient results.

Loop Shaping is a graphical design technique. In this design technique particular shape is provided to magnitude plot of loop transfer function L(s) as per the requirements. This paper presents the approach for designing controller for IBC transfer function G(s) which is given in Eq. (28). This system has a right side zero at ω =1238 rad/s. The main consideration while designing controller for NMP system is right side zero should not get cancelled by controller

ISBN: 978-988-14048-8-6
ISSN: 2078-0958 (Print); ISSN: 2078-0966 (Online)

TABLE II: Design Requirement of Interleaved Boost Converter

Parameters Description	Notations	Experimental Value	Units
Source voltage	V_s	30	V
Output voltage	V_o	50	V
Source current	I_s	1.6667	A
Current through inductor L1	i_{l1}	0.833	A
Current through inductor L2	i_{l2}	0.833	A
Output current	I_o	1	A
Duty ratio	D/d	0.4	-
Switching frequency	f_s	50	KHz
Inductor L1 ripple current	$\triangle I_{l1}$	0.0083	A
Inductor L2 ripple current	$\triangle I_{l2}$	0.0083	A
Voltage ripple	$\triangle V_o$	0.5	V
Inductor	L1	28.91	mH
Inductor	L2	28.91	mH
Capacitor	C	4	μF
Load Resistance	R	50	Ω

transfer function K(s) in order to maintain internal stability of the system [21]. Thus the transfer function of the plant with controller must contain the right side zero. This right side zero also limits the achievable bandwidth, therefore the crossover region should be before ω =1238 rad/s.

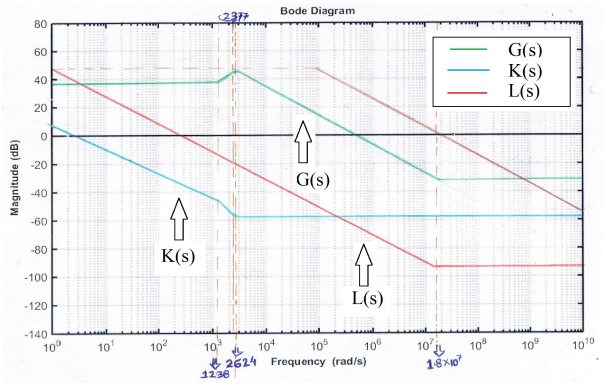

Fig. 3: bode magnitude plot curve with loop shaping

The magnitude plot of plant G(s) is drawn in Fig. 3. The gain crossover frequency is 400000 rad/s. As mentioned above, crossover frequency should be less than ω =1238 rad/s, therefore, in order to get gain crossover frequency as desired, author is using Loop Shaping technique. Here author has reshaped the magnitude plot of G(s) to get the desired magnitude plot of L(s). To fulfill this design requirement a line of -20 dB/dec is plotted for five decades as shown in Fig. 3. The new magnitude plot of L(s) which comprises plant and controller is obtained by drawing a parallel line to above mentioned -20 dB/dec line. This slope is drawn from 1 rad/s to 10^5 rad/s and after that it follows the same slope of G(s). The plot of K(s) is drawn using plot of G(s) and L(s). The controller transfer function K(s) is computed from its magnitude plot and given in Eq. (30). The transfer function of L(s) is computed from K(s)*G(s) and given in Eq. (29).

$$L(s) = \frac{206.2(1 + s/1.78 * 10^7)(1 - s/1.2 * 10^3)}{s(1 + s/1.2 * 10^3)} \quad (29)$$

$$K(s) = \frac{2.5(1 + s/2.3 * 10^3)(1 + s/2.6 * 10^3)}{s(1 + s/1.2 * 10^3)} \quad (30)$$

IV. Results & Discussion

This section deals with the time response and frequency response analysis of IBC using MATLAB. This section also presents the real-time HIL results of IBC using Typhoon HIL 402 device.

A. Time and Frequency Response Analysis

The bode plot of the plant G(s) is shown in Fig. 4. It is clear from the figure that plant behaviour is unstable with gain margin -38.4 dB and phase margin -87.8°. To stabilize it controller has been designed using loop shaping concept as mentioned in previous section.

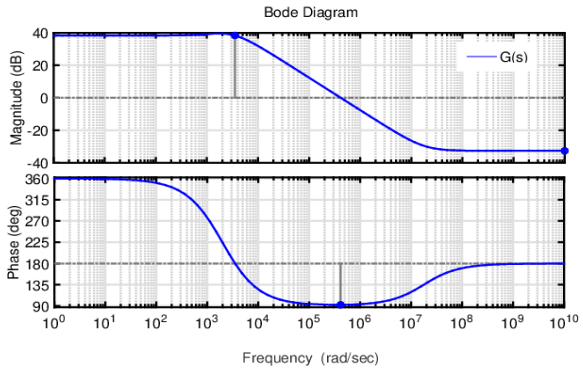

Fig. 4: Bode plot of G(s)

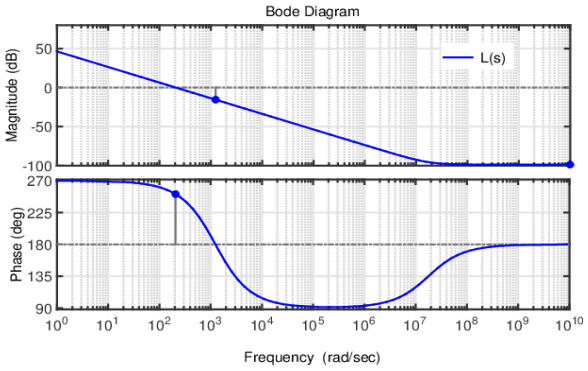

Fig. 5: Bode plot of L(s)

The designed controller K(s) has stabilized the plant with GM and PM 15.8 dB and 71.6° respectively which is shown in Fig. 5.

ISBN: 978-988-14048-8-6
ISSN: 2078-0958 (Print); ISSN: 2078-0966 (Online)

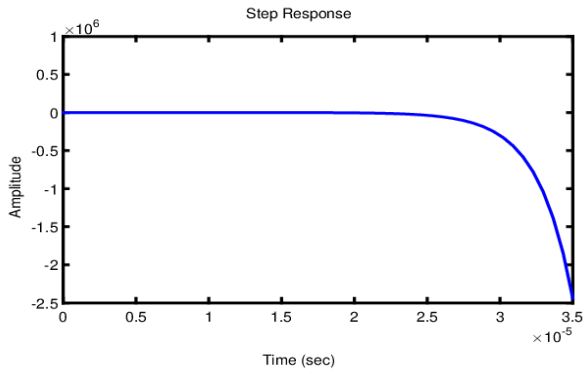

Fig. 6: step response of G(s)

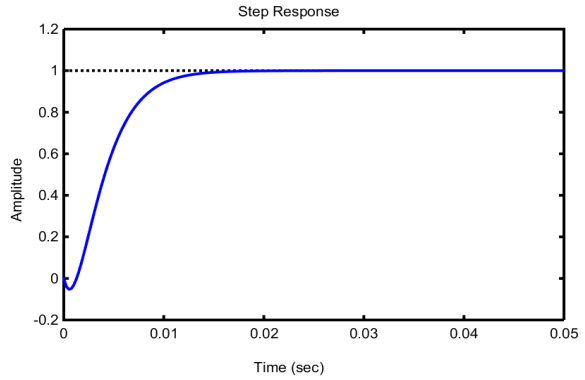

Fig. 7: step response of L(s)

The step response for the G(s) and L(s) are given in Fig. 6 and Fig. 7. Fig. 6 shows the unstable behaviour in step response for open loop IBC. It is observed from Fig. 7 that the system shows the over-damped response with settling time 0.0126 sec.

B. HIL Results using Typhoon 402

Typhoon HIL is an experimental emulator platform which verifies and tests the IBC in real time through virtualization. Fig. 8 is showing the HIL setup which contains digital storage oscilloscope, HIL 402 unit and power circuit model on Typhoon HIL software.

Fig. 8: Hardware in-the-loop experimental setup

Fig. 9 and Fig. 10 is demonstrating the HIL results of IBC for open loop. Channel 1 is showing the input voltage while Channel 2 is showing the output voltage. It is observed from Fig. 9, with change in input voltage, the output voltage is also changing, and the desired output 50V is achievable only

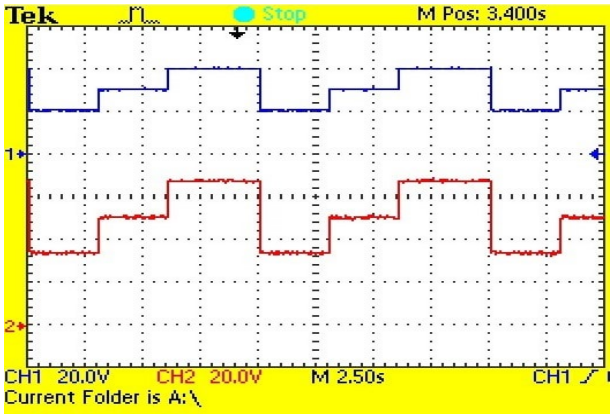

Fig. 9: HIL result of input and output voltage for open loop

when input voltage is 30V. Fig. 10 is showing the inductor currents where Channel 1 is showing i_{l1} while Channel 2 is showing i_{l2}.

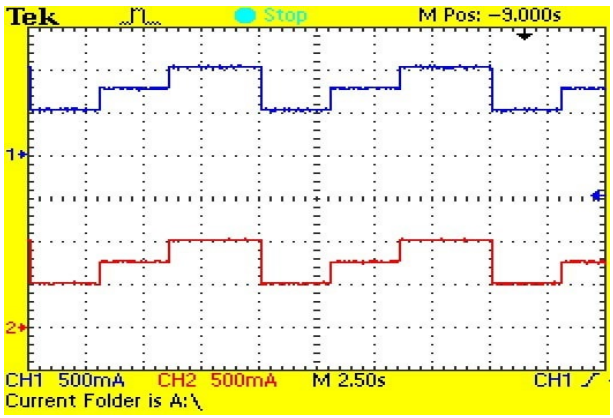

Fig. 10: HIL result of inductor currents for open loop

Fig. 11 is showing the closed loop voltage HIL results. Channel 1 is showing the input voltage while Channel 2 is showing the output voltage. It is observed from the Fig. 11 that the output voltage is maintained constant (50V), irrespective of the Variation in input voltage. Hence the objective of the controller is achieved.

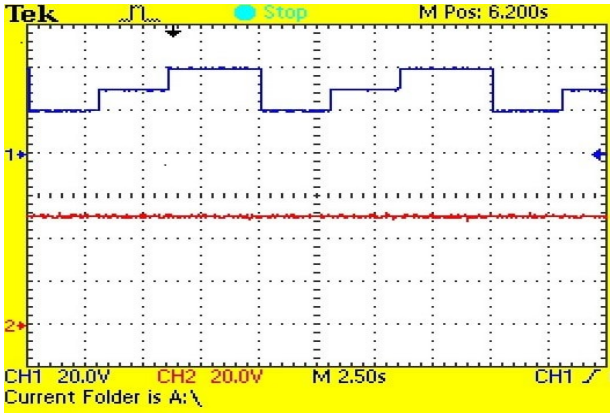

Fig. 11: HIL result of input and output voltage for closed loop

Fig. 12 is showing the inductor currents for closed loop, Channel 1 is showing average current for inductor L1 while Channel 2 is showing average current for inductor L2.

ISBN: 978-988-14048-8-6
ISSN: 2078-0958 (Print); ISSN: 2078-0966 (Online)

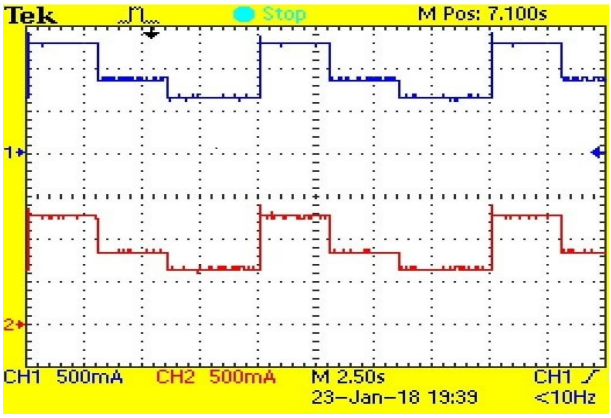

Fig. 12: HIL result of inductor currents for closed loop

V. Conclusion & Future Scope

In this paper, a loop shaping controller has been designed for IBC to get a constant output for variable input. The mathematical modelling of IBC has been presented using state space averaging technique & small signal analysis. Step response and frequency response of open loop & closed loop is analyzed through MATLAB to validate the stability of the system. It has been found that the PM of the closed loop system is 71.1^0, which shows the robustness of the proposed controller. At the end, the HIL responses in digital storage oscilloscope are presented. The closed loop response of IBC is showing the constant output for variable input which shows the efficiency of the proposed controller.

Based on the literature survey, some related issues for future research works are outlined as follows:

- It is worth noting that no controller based on loop shaping technique has been designed for interleaved boost converter in the literature. Therefore standalone unit of loop shaped controller for IBC should be further carried out.
- In the present study linearized control scheme has been used to design converter as well as controller. However, some typical approaches for non linear analysis of power converters can be used such as Floquet theory[22], Lyapunov-based methods[23], trajectory sensitivity approach[24].

References

[1] C.N.M. Ho, H.Breuninger, S.Pettersson, G.Escobar, and F. Canales,"A comparative performance study of an interleaved boost converter using commercialized Si and SiC diodes for pv applications,"8th International Conference on Power Electronics - ECCE Asia, The ShillaJeju, Korea,May 30-June 3, 2011.

[2] M.T.Zhang, M.M.Jovanovic and F.C.Y.Lee, "Analysis and Evaluation of Interleaving Techniques in Forward Converters," IEEE Transactions on Power Electronics, Vol. 13, No.4, pp. 690-698, 1998.

[3] L. Balogh and R. Redl, "Power-factor correction with interleaved boost converters in continuous-inductor-current mode," in Applied Power Electronics Conference and Exposition, 1993. APEC'93. Conference Proceedings 1993., Eighth Annual. IEEE, pp. 168-174, 1993.

[4] H.M.M. Swamy,K.P.Guruswamy, and S.P.Singh, Design, Modeling and Analysis of Two Level Interleaved Boost Converter. 2013 International Conference on Machine Intelligence and Research Advancement 2013.

[5] H.Kosai, S.McNeal, A.Page, B.Jordan, J.Scofield and B.Ray, "Characterizing the effects of inductor coupling on the performance of an interleaved boost converter," in CARTS USA, pp. 168-174, 2009.

[6] B.Converters, "Interleaving is Good for Boost Converters, Too,", Page.1-7, 2008.

[7] A. Newton, T. C. Green, and D. Andrew, " AC/DC Power Factor Correction Using Interleaving Boost and Cuk Converters," in IEEE Power Electronics and Variable Speed, Conference Publication, No.475, Page 293-298, 2000.

[8] B. A. Miwa, D. M. Otten, and M. F. Schlecht, "High Efficiency Power Factor Correction Using Interleaving Techniques,"IEEE Applied Power Electronics Conference and Exposition, Page.557-568, 1992.

[9] S.Banerjee, A.Ghosh and N.Rana,"An Improved Interleaved Boost Converter with PSO-Based Optimal Type-III Controller,"vol. 5, pp 323-337, 2017.

[10] H.Sartipizadeh, and F.Harirchi,"Robust Model Predictive Control of DC-DC Floating Interleaved Boost Converter under Uncertainty", pp 320-327, 2017.

[11] T.Ahmed,K.Nishida and M.Nakaoka,"Analog controller for home application of photovoltaic system using interleaved DC-DC converter and single-phase inverter", Journal Article on Proceedings of the International Conference on Power Electronics and Drive Systems, vol.2015-August, pp. 313-319, 2015.

[12] Y. Huangfu, S. Zhuo and F. Chen,"Evaluation and fault tolerant control of a floating interleaved boost converter for fuel cell systems," in IEEE Transactions on Industry Applications, pp. 1-7, 2016.

[13] R. W. Erickson, and D. Maksimovic, "Fundamentals of power electronics" Springer, 2007.

[14] K. Ogata, "Modern Control Engineering" Pearson Education, India, 2010.

[15] P.Karthika,A.M and P.Ayyapan,"PV Based Speed Control of Dc Motor Using Interleaved Boost Converter With Sic MOSFET and Fuzzy Logic Controller," International Conference on Communication and Signal Processing, pp. 1826-1830, 2016.

[16] Y.Adachi,Y.Mochizuki and K.Higuchi,"Approximate 2DOF digital controller for interleaved PFC boost converter", Journal Article on Lecture Notes in Electrical Engineering, vol.282 LNEE, pp. 135-144, 2014.

[17] S.Banerjee, A.Ghosh and N.Rana,"Design and fabrication of closed loop Two-Phase Interleaved Boost Converter with Type-III controller", pp 3331-3336, 2016.

[18] A.H.M.A. Rahim and M.F. Kandlawala,"Robust STATCOM voltage controller design using loop-shaping," Electric Power Systems Research 68 (2004), pp 61-74, Dhahran, Saudi Arabia, 2003.

[19] R.Cisneros , M.Pirro, G.Bergna ,R.Ortega,G.Ippoliti and M.Molinas, "Global tracking passivity-based PI control of bilinear systems: Application to the interleaved boost and modular multilevel converters," Control Engineering Practise , vol. 43, pp 109-119, 2015.

[20] M. Bougrine, M.Benmiloud,A.Benalia,E.Delaleau and M.Benbouzid , "Load estimator-based hybrid controller design for two-interleaved boost converter dedicated to renewable energy and automotive applications," ISA Transactions, vol.66, pp 425–436, 2017.

[21] Sigurd Skogestad and Ian Postlethwaite, "Multivariable Feedback Control Analysis and Design," Wiley, 2001.

[22] D. Giaouris, S. Banerjee, B. Zahawi, and V. Pickert, "Stability analysis of the continuous-conduction-mode buck converter via Filippov's method," IEEE Trans. Circuits Syst. I, Reg. Papers, vol. 55, no. 4, pp. 1084–1096, May 2008.

[23] S. K. Mazumder and K. Acharya, "Multiple Lyapunov function based reaching condition for orbital existence of switching power converters," IEEE Trans. Power Electron., vol. 23, no. 3, pp. 1449–1471, May 2008.

[24] I. A. Hiskens and M. A. Pai, "Trajectory sensitivity analysis of hybrid systems," IEEE Trans. Circuits Syst. I, Reg. Papers, vol. 47, no. 2, pp. 204–220, Feb. 2000.

ISBN: 978-988-14048-8-6
ISSN: 2078-0958 (Print); ISSN: 2078-0966 (Online)